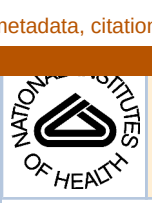

Published in final edited form as:

J Theor Biol. 2007 November 21; 249(2): 361–375. doi:10.1016/j.jtbi.2007.07.025.

A mathematical model for human nucleotide excision repair: damage recognition by random order assembly and kinetic proofreading

Kevin J. Kesseler[1], **William K. Kaufmann**[2], **Joyce T. Reardon**[3], **Timothy Elston**[4], and **Aziz Sancar**[5]

1 *Department of Pathology and Laboratory Medicine, Lineberger Comprehensive Cancer Center, University of North Carolina at Chapel Hill, Chapel Hill, NC 27599-7255, U.S.A., kesseler@email.unc.edu*

2 *Department of Pathology and Laboratory Medicine, Lineberger Comprehensive Cancer Center, Center for Environmental Health and Susceptibility, University of North Carolina at Chapel Hill, Chapel Hill, NC 27599-7255, U.S.A., wkarlk@med.unc.edu*

3 *Department of Biochemistry and Biophysics, University of North Carolina at Chapel Hill, Chapel Hill, NC 27599-7260, U.S.A., joyce reardon@med.unc.edu*

4 *Department of Pharmacology, University of North Carolina at Chapel Hill, Chapel Hill, NC 27599-7260, U.S.A., telston@amath.unc.edu*

5 *Department of Biochemistry and Biophysics, Lineberger Comprehensive Cancer Center, Center for Environmental Health and Susceptibility, University of North Carolina at Chapel Hill, Chapel Hill, NC 27599-7260, U.S.A., aziz sancar@med.unc.edu*

Abstract

A mathematical model of human nucleotide excision repair was constructed and validated. The model incorporates cooperative damage recognition by RPA, XPA, and XPC followed by three kinetic proofreading steps by the TFIIH transcription/repair factor. The model yields results consistent with experimental data regarding excision rates of UV photoproducts by the reconstituted human excision nuclease system as well as the excision of oligonucleotides from undamaged DNA. The model predicts the effect that changes in the initial concentrations of repair factors have on the excision rate of damaged DNA and provides a testable hypothesis on the bio-chemical mechanism of cooperativity in protein assembly, suggesting experiments to determine if cooperativity in protein assembly results from an increased association rate or a decreased dissociation rate. Finally, a comparison between the random order assembly with kinetic proofreading model and a sequential assembly model is made. This investigation reveals the advantages of the random order assembly/kinetic proofreading model.

Keywords

Damage recognition; random order assembly; cooperative binding; kinetic proofreading

Communication: K. J. Kesseler kesseler@email.unc.edu

1. Introduction

Nucleotide excision repair (excision repair) is an intracellular process which repairs damaged DNA. Repair factors assemble at a lesion on the DNA to form a complex that excises a short segment of DNA which contains the damaged base. After the damaged oligomer is removed, additional proteins join the complex to replace the excised section of DNA.

We developed a mathematical model for human nucleotide excision repair. The model was used to simulate both *in vitro* and *in vivo* experiments that involve both cyclobutane pyrimidine dimers (Pyr<>Pyr) and pyrimidine-pyrimidone 6–4 photoproducts [(6–4) photoproducts] as substrates. The mathematical model is based on biochemical data from recent *in vitro* studies ([19],[25],[20]) on damage recognition by, and the order of assembly of, the human excision nuclease system. Excision repair in humans is initiated by the coordinated action of six repair factors, RPA, XPA, XPC, TFIIH, XPG, and XPF·ERCC1, these repair factors remove damaged nucleotides in the form of 24–32-nt-long oligomers that are generated by dual incisions at the 20^{th} ± 5 phosphodiester bond 5′ and the 6^{th} ±3 phosphodiester bond 3′ to the damage [10].

Two models have been proposed for the assembly of the nuclease that produces the dual incisions. In one model the damage is recognized by RPA, XPA, or XPC first and the other factors assemble in a rigid sequential order ([22], [24], [25], [18]). In the second model the three damage recognition factors, RPA, XPA, and XPC, assemble at the damage site in a random order but cooperatively, and the specificity conferred by these factors is enhanced by the kinetic proofreading activity of TFIIH to achieve a physiologically relevant specificity [19]. According to the random order-cooperative binding/kinetic proofreading model the reaction proceeds as follows (Figure 1): RPA, XPA, and XPC·TFIIH (a major fraction of XPC is in a complex with TFIIH *in vivo* ([2], [13])) bind to the damage site in random order and recruit the other damage recognition factors by protein-protein interactions that increase the specificity by cooperative assembly. Then, the XPB and XPD subunits of TFIIH, which are ATP-dependent DNA helicases, hydrolyze ATP to make a relatively stable complex called pre-incision complex 1 (PIC1). Within this complex the DNA is unwound by about 20 bp around the damage site and is kinked in the vicinity of the damage [14]. Then, in a reaction that is dependent on ATP hydrolysis by TFIIH, XPG enters the complex and XPC is released to form PIC2. Finally, in a third step that requires ATP hydrolysis by TFIIH, XPF·ERCC1 enters PIC2 to form PIC3 [14]. Within PIC3 XPG makes the 3′ incision and XPF·ERCC1 makes the 5′ incision and the excised oligomer and the repair factors, with the exception of RPA, dissociate from the gapped duplex.

Excision repair has an essentially limitless substrate range. It acts on lesions such as (6–4) photoproducts that distort the helix drastically, on Pyr<>Pyr that makes more subtle structural changes in DNA, on methylated purines and reduced pyrimidines that cause yet subtler structural changes, and even on undamaged DNA ([9],[1]). Many of these lesions including the classic substrate for excision repair, the Pyr<>Pyr, cannot be discriminated from undamaged DNA by the three damage recognition factors, RPA, XPA, and XPC [19]. Therefore, it was proposed that the physiologically relevant specificity could be achieved only by the cooperativity of the three damage sensors combined with kinetic proofreading activity of TFIIH ([19], [20], [24]). Moreover, because of attack by the enzyme system even on undamaged DNA, it was proposed that the major determinant of specificity was kinetic proofreading.

In the classical kinetic proofreading scheme for biological reactions the initial binding of cognate and non-cognate substrates is at a rate dictated by the respective free energies of binding. Following this, one or more irreversible steps are introduced between the initial binding and the ultimate catalysis step. Importantly, the irreversibility of the intermediate step

(s) is achieved by a coupled ATP hydrolysis reaction and the reaction may be aborted at each step not to the preceding precursors but to the initial reactants. The net effect of this reaction scheme is to achieve specificity approximating that which can be achieved by the n^{th} power of the initial free energy of binding ([8],[15]).

2. Model Formulation and Numerical Methods

Within the overall constraints of the biochemical features of human excision repair we have developed a mathematical model for the repair system. The model assumes that the three damage sensors, RPA, XPA, and XPC (which we assume to be associated with TFIIH), bind at random locations on the DNA. Each of these proteins is assumed to have higher affinity for damaged DNA manifested by a slower dissociation rate constant relative to undamaged DNA. In addition, the model assumes cooperativity among these repair factors; that is, if two or more repair factors are bound to the same location on the DNA then these repair factors are less likely to dissociate than if there were only one repair factor bound in that location. As the mechanistic details of kinetic proofreading in excision repair are not fully understood, that part of the model is formulated to match the experimental repair rate values rather than modeling the actual physical intermediates.

It should be noted that we have used a deterministic model for this study. While stochastic effects may be significant in nucleotide excision repair *in vivo*, the current study focuses primarily on *in vitro* studies in which the molecular numbers are sufficient to justify using a deterministic ODE model.

2.1. Model

Excision repair has been modeled as follows. The various DNA complexes involved from DNA alone to DNA with the repair factors XPA, XPC-TFIIH and RPA bound to it (the direct precursor of pre-incision complex 1 (PIC1)) as well as pre-incision complexes 1–3, are shown in Figure 2. In the model, there are several variants of this schematic – one for undamaged DNA, one for damaged DNA, and one for damaged DNA where the location of the assembling repair factors does not include the DNA lesion. There could be other variants of this schematic if a simulation involved two types of DNA damage. The random order assembly of the repair factors RPA, XPA, and XPC-TFIIH is modeled by reversible mass-action kinetics. It is assumed that each of the repair factors binds to DNA at a rate proportional to the product of the concentrations of the DNA complex and the repair factor that is binding to it. If forward cooperativity is used in the model, then a scale factor multiplies the forward rate constants for subsequent binding events as explained below. It is also assumed that repair factors dissociate from complexes at a rate proportional to the concentration of that complex. In the event that backward cooperativity is used in the model, the scale factor multiplies the rate constants for dissociation as explained below. The rate constants for the different repair factors binding to DNA is assumed to be equal and thus do not depend on either the repair factor in question or the complex to which it is binding. This constant (κ_{on}) is assumed to be $10^6 M^{-1} s^{-1}$. The rate constants for the dissociation of repair factors are model parameters and depend on both the repair factor which is dissociating and the type of lesion from which it dissociates. These dissociation constants were determined experimentally [19] and are different for damaged versus undamaged DNA and for the 6 –4 photoproducts and the *T* <> *T* cyclobutane pyrimidine dimer.

The other factor that can affect the binding rate or dissociation rate of repair factors is cooperativity – the increased stability of a complex that includes two or more repair factors. Two different methods for modeling cooperativity have been employed in this model. Forward cooperativity increases the binding rate of repair factors to complexes that already include one or more repair factors and backward cooperativity decreases the dissociation rate of repair

factors from complexes that contain at least two repair factors. Forward cooperativity is modeled by multiplying the association rate of repair factors binding to complexes that include exactly one other repair factor by a cooperativity constant (κ^{f}_{coop}) and multiplying the association rate of repair factors binding to complexes that include both of the other repair factors by $(\kappa^{f}_{coop})^{2}$. Backward cooperativity is modeled by multiplying each term that represents dissociation from a complex that includes two repair factors by a cooperativity constant (κ^{b}_{coop}) and multiplying the terms representing dissociation from a complex that includes all three repair factors by $(\kappa^{b}_{coop})^{2}$. For information on the energy constraints on modeling cooperativity see the Appendix. κ^{f}_{coop} is greater than 1 and κ^{b}_{coop} is smaller than 1, i.e. forward cooperativity makes binding **more** likely and backward cooperativity makes dissociation **less** likely. While it is assumed that cooperativity plays a significant role in the reaction rates of the repair factors, we lack the experimental data necessary to determine the type of cooperativity or the cooperativity constant, leaving it as an open parameter to use to fit the model to the data.

All of the reactions involving the association of the repair factors RPA, XPA and XPC-TFIIH are reversible. The complex that contains all three repair factors, however, may undergo kinetic proofreading whereby ATP hydrolysis may either dissociate all 3 repair factors or lead to the stable binding of the repair factors at the damage site (PIC1 complex). The rate at which this step takes place (k_1) is unknown, again providing a parameter that may be used to fit the model. PIC1 may then progress to PIC2 and then PIC3 where ATP hydrolysis is employed a second and third time to discriminate substrate from non-substrate to achieve the final specificity. It must be noted that kinetic proofreading by its very nature is not absolute, and non-substrate (undamaged) DNA does proceed through all the thermodynamic and kinetic selection processes and is subjected to the irreversible dual incision reaction. The second kinetic proofreading step is triggered (in the model) by the binding of XPG to PIC1 and results in PIC2 or dissociation and the last step is triggered by the binding of XPF·ERCC1 to PIC2 and yields PIC3 if the complex is not dissociated. If the PIC3 complex is reached, then excision is assumed to have taken place and the DNA is considered repaired following rapid gap-filling DNA synthesis by DNA polymerase ε/δ and DNA ligation (by DNA Ligase I) to restore the original full duplex DNA structure.

Once the first kinetic proofreading step occurs the process is irreversible and ultimately results in either dissociation of the entire complex or excision of the DNA. Kinetic proofreading is represented in the model by assuming that all three kinetic proofreading steps have a fixed probability of dissociating the complex depending on whether the DNA is damaged or not (but **not** depending on the type of DNA damage). These probabilities provide more parameters which may be used to adjust the fit of the model. The parameters used in the model and typical values for them are listed in Table 1. κ^{on}, the rate at which all repair factors bind to DNA, is assumed to be the same for all repair factors and DNA complexes. The value of this constant is set by experimental data [19]. The parameters of the form $\kappa^{*off}_{\#}$, where (*) is a type of DNA complex (undamaged, T<>T lesion, or (6 – 4) lesion) and (#) is one of the three repair factors (RPA, XPA, or XPC), are the dissociation constants. They give the rate at which the repair factors dissociate from DNA complexes and their values are set by experimental data [19]. The parameter Pr_{hit} is the probability that a repair factor associating with a damaged DNA complex binds to the lesion (as opposed to the undamaged portion of the DNA). This parameter is set by the geometry of the system (i.e. the relative sizes of the DNA, the lesions, and the repair complex). The cooperativity constant κ_{coop} determines the strength of cooperativity between repair factors and, as described above, it is a free parameter. k_1, as described above, is the rate at which DNA complexes with all three repair factors undergo kinetic proofreading (resulting

in either PIC1 or dissociation of the complex); k_1 is another free parameter. The remaining free parameters k_{Pr}^D and k_{Pr}^U are the probabilities that damaged and undamaged DNA complexes respectively are dissociated by kinetic proofreading. These probabilities are assumed to be the same for each kinetic proofreading step. The differential equations describing this model are given in the second Appendix.

3. Validation

Tables 4 and 5 contain experimental data for excision repair in a reconstituted cell-free system. The tables show the concentrations of repair factors (in nM), incubation time (in minutes), and percentage excision of the lesion in each experiment. All of the experiments were conducted *in vitro* with 0.8 nM of radioactively labeled 136 bp long substrates of DNA with a T<>T dimer (Table 4) or (6–4) photoproduct (Table 5). The reactants were mixed and incubated for the indicated time after which the fraction of DNA lesions that were excised was determined. The model equations were solved using the XPPAUT [3] software package (using various implicit solvers, primarily the backward Euler solver).

To determine the accuracy of the excision repair model the following experiment was performed: The model parameters were tuned so the results agreed with one experimental trial from Table 4 or Table 5. Then simulations of the other experimental trials in the table were run with these parameters. The results of one experiment from Table 4 and three experiments from Table 5 are shown in Figure 3, with the X-coordinate representing the amount of damage excised in the simulation and the Y-coordinate representing the amount of damage excised in the biochemical experiment. As can be seen by these graphs, even this crude method of fitting the data yields reasonable results. In order to better understand the ability of the model to fit the data the following experiment was performed.

The experiments involving the T<>T dimer exhibit more variability because the T<>T dimer is repaired poorly by human excision nuclease and thus experimental error is large with respect to the total amount of damage excised. For this reason, the data for (6–4) photoproduct repair was considered. To measure the fit of the model given a particular parameter set, the equation below was used to determine the normalized error of each simulation:

$$e_{normalized} = \left(\frac{x_{obs} - x_{sim}}{x_{obs}} \right)^2 .$$

The above quantity was summed over seven different runs simulating experiments from Table 5. The results over ranges of the parameter values k_{Pr}^D (0.05 → 0.15) and k_1 (0.01 → 0.11) (the other parameters were fixed) are shown in Figure 4. The parameters k_{Pr}^D and k_1 were chosen because apart from κ_{on}, the value of which is determined experimentally, the model is most sensitive to changes in these two parameters (as shown below). The color represents the sum of the normalized error from each of the seven runs with dark blue representing a total error of 5 (or greater) and dark red representing an error of 0. As can be seen from this figure, there is a broad range of parameter values which yield a reasonable fit to the experimental data (i.e. error is small). Additionally, this fit could be improved by allowing variation of the other parameters as well. An additional result of this study is that as the accuracy of the kinetic proofreading is decreased (k_{Pr}^D is increased), the range of values of k_1 for which the model is a good fit to the data increases.

The sensitivity of the model to changes in parameter values from the baseline parameters was determined. The sensitivity of a parameter is measured by the ratio of the percentage change

in output (in this case the excision rate) to the percentage change in input (the parameter for which the sensitivity is being measured). The results of this study (Table 3) show that the model is most sensitive to the parameter of the forward reaction rate for the association of RPA, XPA, and XPC (k_{On}) with a 1% change in the reaction rate causing nearly a 13% change in excision. This is a reflection of the fact that the rate of assembly of repair factors has the biggest impact on the rate at which excision occurs as this rate governs the speed at which most of the steps in this model occur. The parameter with the second most impact on the model is k_{Pr}^{D}, the probability that kinetic proofreading will dissociate the repair complex from damaged DNA, with a sensitivity of −3.31 (the negative value indicates that an increase in the parameter causes a decrease in the amount of damage excised). As this parameter directly controls the number of lesions proceeding through all three kinetic proofreading steps effectively setting the accuracy of kinetic proofreading, its significant impact on the model is unsurprising. The parameters k_1 (the rate at which the first kinetic proofreading step occurs), Coop (backward cooperativity was used in this study), and Pr^H(the probability that a repair factor binding to damaged DNA binds at the damage site) all have moderate sensitivity values (0.99, 0.65, and 0.44 respectively) which is consistent with the fact that while all of these parameters directly impact the rate at which the excision complexes form; k_1 and Pr^H only affect the model in one location each and the cooperativity constant, while impacting the model at several different locations, affects only the dissociation rates of proteins. As the dissociation rates are small to begin with, the impact of changing them is likewise small. Finally, the parameter k_{Pr}^{U}, the probability that kinetic proofreading dissociates the excision complex from undamaged DNA, has a very low sensitivity (0.00875) due to it not affecting the excision of damaged DNA, but rather the rate at which excision complexes are dissociated from undamaged DNA.

Figure 5 shows simulations that model three experimental results described in Figure 3 from [19]. The experiment (in [19]) was used to determine the dissociation constants for the various repair factors. The simulation shows how well our method of modeling the association/dissociation of repair factors agrees with the experimental results for RPA, XPA, and XPC. It should be noted that there was no attempt made to fit these curves to the data, instead the dissociation constant determined by the experiment was used in the model. If the dissociation constants used in the model were chosen to better fit these curves, the overall fit of the model would most likely be improved.

Additional studies examined the effect on damage excision of varying the concentration of the repair factors RPA, XPA, and XPC-TFIIH. A series of runs were generated where the concentration of one of the repair factors was varied from 10^{-4} times to 10^{2} times the baseline value while the concentrations of the other repair factors was held fixed. The y-axis is a log scale varying from $10^{-3}nM$ to $5 \times 10^{-2}nM$. The baseline values for all of these experiments were $[RPA] = 200nM$, $[XPA] = 50nM$, and $[XPC] = 5nM$. These baseline values were those used in experiment 3C from table 5. Figure 6 shows that the effects of varying the concentrations of the different repair factors are qualitatively similar with the differences in the three graphs mainly due to differences in the baseline concentrations of the repair factors.

Many numerical simulations were performed to validate the model and to illustrate its behavior. In several of the simulations, the following method was used: the model was run for concentrations of the primary repair factors (generally) ranging from 10^{-2} to 10^{2} times a set of baseline values (200*nM* RPA, 50*nM* XPA, and 5*nM* XPC). This experiment was then repeated with different configurations of the model, different concentrations of the repair factors, or different parameter values. The results showed the effects of various changes in the model on the excision rate under conditions ranging from limited repair factors to an excess of repair factors.

Analyses of excision repair *in vitro* suggest that repair factors cooperate in the excision of damaged DNA. Two different ways of modeling cooperativity in the assembly of repair factors were investigated. Forward cooperativity implies that the binding of a repair factor to a DNA complex is more likely if other repair factors are already present in the complex. Backward cooperativity implies that the dissociation of a repair factor from a DNA complex is less likely if other repair factors are present in the complex. Figure 7 shows the effect of varying the cooperativity constant on the amount of DNA excised for both the forward and backward cooperativity cases. From the forward cooperativity experiment the excision rate ranged from relatively low values for limiting concentrations of repair factors (left side of the upper right panel of Figure 7) to relatively high values for excessive concentrations (right side of the upper right panel of Figure 7). The cooperativity constant controls where this jump from low to high excision occurs. For values (of the cooperativity constant) roughly between 1 and 10 the location of this jump varies significantly, while the location of this jump is fairly insensitive to changes in the cooperativity constant between 10 and 100. The results from the backward cooperativity experiment are qualitatively very similar to the results from the forward cooperativity experiment. The most significant difference between the two being that with backward cooperativity the rate of excision increases to a local maximum before decreasing to an asymptotic value as the concentration of repair factors is increased, while with forward cooperativity excision rate increases monotonically to an asymptotic maximum rate. This suggests that the type of cooperativity seen (forward or backward) can be experimentally determined by the shape of the curve of DNA excision vs. concentration of repair factors. Specifically, as the concentration of repair factors is increased, does excision rate increase monotonically to an asymptotic maximum value indicating forward cooperativity or does it increase to a local maximum and then decrease to an asymptotic value indicating backward cooperativity? Examples of these curves for forward (red) and backward (blue) cooperativity are shown in the lower left panel of Figure 7. These experiments are currently in progress in our lab.

4. Comparision to other models

In a recently published paper [16] a mathematical model of excision repair was proposed involving sequential (rather than random order) binding of the repair factors to DNA lesions. It was shown in that study that sequential binding can account for the rate at which excision occurs in *in vivo* experiments. There are, however, several aspects in which the model proposed in the current study provides additional detail and a more general context than its predecessor. First, the sequential model did not include the repair factor RPA, which has been shown ([13],[7], [26]) to be essential for the dual incision step. Furthermore, the sequential model assumes that the repair factors assemble only at locations on the DNA where damage has occurred with no possibility of error whereas the current model incorporates repair factors assembling on undamaged DNA, DNA lesions, and additionally at incorrect (undamaged) areas on pieces of damaged DNA, thus allowing the model to be applied in more general circumstances. Finally, the sequential model did not include any mechanism for kinetic proofreading, further limiting its versatility.

In order to investigate the difference between random order assembly of the repair factors (RPA, XPA, and XPC binding in any order) and sequential assembly, four additional models were created (plus the original random order assembly model) and an experiment was run in which the concentrations of all three repair factors were varied from $10^{-2} \rightarrow 10^{2}$ times the baseline values of 200nM RPA, 50nM XPA, and 5nM XPC. In the first model the order of binding of the repair factors was required to be RPA first, then XPA and XPC last. The second model was totally sequential as well, with the order of binding being XPC followed by XPA and then RPA. The other two models were both hybrids, with both random order and sequential steps. In the third model, RPA was required to be the first repair factor to bind, but then XPA

and XPC were free to bind in either order. Similarly, in the fourth model, XPC was required to bind first and then RPA and XPA were allowed to bind in either order. Figure 8 shows the results of these experiments. The order of assembly for the 4 new models was: (1) RPA → XPA → XPC; (2) XPC → XPA → RPA; and (3) RPA → XPA or XPC → XPC or XPA; (4) XPC → RPA or XPA → XPA or RPA. (The 5th model was the random order assembly model.) The curves on the figure are the results of model (1) - purple, model (2) - blue, model (3) - red, model (4) - green, and model (5) - black. This experiment shows that when the concentrations of the repair factors are below the baseline values, the random order assembly model yields the highest excision rate; when the concentrations are near the baseline value, the models in which the most abundant repair factor (RPA) binds first (1 and 3) are favored slightly over random order assembly (5) and strongly over the model in which the least abundant repair factor (XPC) is bound first (2). As the concentration of repair factors is increased above the baseline values, the excision rate in all four models appears to approach the same asymptotic excision rate.

Figure 9 shows the result of a similar experiment in which each of the models in the preceding experiment were made one-way (once bound, repair factors were not allowed to dissociate from the DNA complex). As can be seen in Figure 9, all 5 one-way models exhibit nearly identical behavior. From these two studies it is apparent that not only did the one-way models lose the range of behaviors seen in the case where reactions in both directions are allowed but they also produced lower excision rates than the full model for most concentrations of repair factors.

5. Discussion

Nucleotide excision repair is the sole repair system for carcinogenic UV-induced DNA photoproducts, the cyclobutane pyrimidine dimer and (6–4) photoproduct, as well as other bulky DNA lesions induced by numerous chemical agents including benzo[a]pyrene, cisplatin, psoralen, and N-acetoxy-N-acetylaminofluorene. In addition, excision repair plays a backup role for base excision repair as it has been found to act on non-bulky substrates normally processed by other pathways ([1],[9],[17]). The reaction is carried out by six repair factors, RPA, XPA, XPC, TFIIH, XPG, and XPF·ERCC1 ([13],[21]). It is well established that RPA, XPA, and XPC are involved in damage recognition, TFIIH in unwinding the DNA around the damage, and XPG and XPF·ERCC1 in the 3′ and 5′ incisions, respectively. However, the order of assembly of these six repair factors is a matter of some debate.

It should be noted that both our experimental and theoretical approaches have dealt with naked DNA and repair proteins. In vivo, the DNA is in nucleosomes and higher order DNA packing structures. This packing limits the access of the repair factors to DNA ([4],[5]). However, this fact does not alter the main conclusions of the paper because packing of DNA into chromatin reduces the accessibility of both damaged and undamaged DNA similarly, with the end result of a somewhat slower rate of repair without a significant change in selectivity which is defined as the ratio of the probability of binding of a repair factor to a damaged site to the probability of binding to an undamaged site. Indeed, a recent study using a novel method to detect damage binding of the human excision repair factors to damage in chromatin in vivo ([11],[16]) has provided direct evidence for the random order assembly model of human excision repair.

Two models have been advanced for the assembly of the six repair factors: the “sequential assembly” model and the model of “random order assembly/kinetic proofreading”. In the sequential model, it has been proposed that XPA [12], RPA [18], the RPA-XPA complex [25], or XPC [22] bind to the damage site first and then the other factors assemble in a rigid order. In the random order assembly/kinetic proofreading model, RPA, XPA, or XPC-TFIIH may bind to the damage first and, regardless of which of the three is bound first, protein-protein

interactions among the three facilitate the assembly of the RPA-XPA-XPC-TFIIH complex and improves specificity ([19], [20]). In this model, the specificity is further improved by kinetic proofreading whereby, following the initial 4-factor assembly, the DNA is unwound around the damage by TFIIH and XPG and XPF·ERCC1 are recruited in three structurally and kinetically distinct steps.

While the repair of the (6–4) photoproduct and other highly efficient substrates is consistent with either model, the repair of the major UV photolesion, the cyclobutane pyrimidine dimer, cannot be accommodated by the sequential assembly model because none of the three damage sensors can measurably discriminate between Pyr<>Pyr and undamaged DNA and, indeed, one study reported that XPC prefers undamaged DNA over Pyr<>Pyr [6]. Despite such limitations, the ordered assembly model in which XPC is the damage sensor that constitutes the nucleation site for the other repair factors has gained some support from several experimental observations. First, among the three damage sensors XPC has the highest affinity to (6–4) photoproducts and other lesions that are repaired with high and comparable efficiencies ([19], [22], [25]). Second, in assays using micropore irradiation followed by immunostaining for UV photoproducts and repair factors it was reported that XPC was recruited to the damage/photoproduct foci in the absence of XPA and XPA was undetectable in these foci in the absence of XPC [23]. Finally, a recent stochastic mathematical model for excision repair based on the sequential assembly model yielded theoretical rates of repair consistent with the *in vivo* experimental data and furthermore concluded that the random order assembly model was not consistent with the *in vivo* experimental data because the random order assembly model would result in slower kinetics of excision than experimentally determined [16].

However, both the experimental and theoretical evidence used to support the sequential assembly model with XPC as the damage sensor have serious shortcomings. First, results of the order-of-addition experiments whereby it was reported that incubation with XPC first yields faster rates of repair compared with rates obtained when substrate is incubated with RPA plus XPA [22] have not been confirmed ([19], [24]). Second, there is no evidence that XPC can discriminate undamaged DNA from DNA with T<>T and yet the reconstituted human excision nuclease repairs T<>T at a relative rate comparable to the *in vivo* rate ([19], [20]). Third, the micropore UV irradiation-induced XPC foci that do form in the absence of XPA may conceivably form by recruitment of XPC by damage-bound RPA. However, under the assay conditions RPA foci are not detectable even though it is known that RPA is required for assembly of the human excision nuclease [13]. Fourth, the report that XPA is not recruited to UV damage sites in the absence of XPC based on mircopore irradiation foci formation [23] has recently been contradicted by the higher resolution chromatin immunoprecipitation assay that shows both RPA and XPA are recruited to the site of damage in the absence of XPC [11].

Regarding the mathematical model that arrives at the conclusion that the human excision nuclease must assemble by the sequential model [16], the model ignores some physico-chemical facts that cast serious doubts about the applicability of the model to the biochemical question at hand. First, there are protein-protein interactions among the three damage sensors, RPA, XPA, and XPC, and these interactions will inevitably lead to a cooperative mode of assembly. Second, the sequential assembly model compared rates of repair under conditions where XPA could bind to the damage site independent of other factors (random) and concluded that under the former conditions the rate of repair would be faster and more consistent with the *in vivo* rate of repair because under the latter conditions XPA (as well as RPA), especially in the presence of high levels of DNA damage, would be sequestered at different lesions effectively reducing the concentration of the proteins available for co-assembly. While, undoubtedly, this logical argument sounds attractive, in reality it is a teleological argument that does not take into account the physico-chemical properties of these proteins: preferential

binding to damaged DNA is an intrinsic property of RPA and XPA ([19],[25]). Whether their independent binding would slow down the eventual assembly of the excision complex, these proteins will bind to damaged DNA independent of XPC and greater fractions of both proteins will be bound to damage without XPC with increasing damage concentration. Any mathematical model aimed at reconstructing excision repair must incorporate this physico-chemical reality. Third, the sequential assembly mathematical model does not take into account the high affinity binding of XPC to undamaged DNA ([17],[25]) nor the fact that the human excision nuclease excises undamaged DNA at a low but biologically significant level ([1], [20]). Finally, the sequential assembly model ignores the specificity that is conferred by kinetic proofreading which is quite likely the major source of specificity in human excision repair.

The mathematical model we present in this paper, in contrast, takes into account all of the physico-chemical properties of the damage sensors, and it incorporates the relatively high affinity binding of damage sensors to undamaged DNA and the attack of undamaged DNA by the human excision nuclease ensemble. Most importantly, our random order binding/kinetic proofreading model is capable of explaining the recognition and repair of lesions such as Pyr<>Pyr that are not discriminated from undamaged DNA as measured by conventional DNA binding assays. We propose that in the case of the (6 – 4) photoproduct the thermodynamic recognition coupled with cooperativity plays a prominent role whereas in the case of T<>T type lesions kinetic proofreading is, by far, the predominant mechanism for achieving specificity. Furthermore, the model suggests that this difference in the random order binding of damage sensors is not sufficient to account for the difference in excision rates of (6–4) and T<>T lesions, indicating that there may be differences in effectiveness of kinetic proofreading on different types of damaged substrates.

Acknowledgments

Supported by grants from the Lineberger Comprehensive Cancer Center (CA16086 to WKK), the UNC Center for Environmental Health and Susceptibility (ES10126 to WKK), and PHS grants ES11391(to WKK) and GM32833 (to AS).

Kevin Kesseler received support from NIH Grant T32CA09156 at the University of North Carolina Lineberger Comprehensive Cancer Center.

Special thanks to Stephanie Hutsell (Department of Biochemistry and Biophysics, University of North Carolina at Chapel Hill) for useful disscussions in early stages of this work.

The programs DataTank and DataGraph were used in the creation of the figures for this paper.

References

1. Branum ME, Reardon JT, Sancar A. DNA repair excision nuclease attacks undamaged DNA. J Biol Chem 2001;276:25421–25426. [PubMed: 11353769]
2. Drapkin R, Reardon JT, Ansari A, Huang J-C, Zawel L, Ahn K, Sancar A, Reinberg D. Dual role of TFIIH in DNA excision repair and in transcription by RNA polymerase II. Nature 1994;368:769–772. [PubMed: 8152490]
3. Ermentrout, B. Simulating, analyzing, and animating dynamical systems: a guide to XPPAUT for researchers and students. SIAM Press; Philadelphia: 2002.
4. Hara R, Mo J, Sancar A. DNA damage in the nucleosome core is refractory to repair by human excision nuclease. Mol Cell Biol 2000;20(24):9173–9181. [PubMed: 11094069]
5. Hara R, Sancar A. The SWI/SNF chromatin-remodeling factor simulates repair by human excision nuclease in the mononucleosome core particle. Mol Cell Biol 2002;22(19):6779–6787. [PubMed: 12215535]

6. Hey T, Lipps G, Sugasawa K, Iwai S, Hanaoka F, Krauss G. The XPC-HR23B complex displays high affinity and specificity for damaged DNA in a true-equilibrium fluorescence assay. Biochemistry 2002;41(21):6583–6587. [PubMed: 12022861]
7. He Z, Henricksen LA, Wold MS, Ingles CJ. Rpa involvement in the damage-recognition and incision steps of nucleotide excision repair. Nature 1995;374:566–569. [PubMed: 7700386]
8. Hopfield JJ. Kinetic proofreading: a new mechanism for reducing errors in biosynthetic processes requiring high specificity. Proc Natl Acad Sci 1974;71:4135–4139. [PubMed: 4530290]
9. Huang J-C, Hsu DS, Kazantsev A, Sancar A. Substrate spectrum of human exinuclease: Repair of abasic sites, methylated bases, mismatches, and bulky adducts. Proc Natl Acad Sci 1994;91:12213–12217. [PubMed: 7991608]
10. Huang J-C, Svoboda DL, Reardon JT, Sancar A. Human nucleotide excision nuclease removes thymine dimers from DNA by incising the 22^{nd} phosphodiester bond 5′ and the 6^{th} phosphodiester 3′ to the photodimer. Proc Natl Acad Sci 1992;89:3644–3688. [PubMed: 1373506]
11. Jiang G, Sancar A. Recruitment of DNA damage checkpoint proteins to damage in transcribed and nontranscribed sequences. Mol Cell Biol 2006;26(1):39–49. [PubMed: 16354678]
12. Mu D, Hsu DS, Sancar A. Reaction mechanism of human DNA repair excision nuclease. J Biol Chem 1996;271:8285–8294. [PubMed: 8626523]
13. Mu D, Park C-H, Masunaga T, Hsu DS, Reardon JT, Sancar A. Reconstitution of the human DNA repair excision nuclease in a highly defined system. J Biol Chem 1995;270:2415–2418. [PubMed: 7852297]
14. Mu D, Wakasugi M, Hsu DS, Sancar A. Characterization of reaction intermediates of human excision repair nuclease. J Biol Chem 1998;273(31):28971–28979.
15. Ninio J. Kinetic amplification of enzyme discrimination. Biochimie 1975;57(5):587–595. [PubMed: 1182215]
16. Politi A, Mone MJ, Houtsmuller AB, Hoogenstraten D, Vermeulen W, Heinrich R, van Driel R. Mathematical modeling of nucleotide excision repair reveals efficiency of sequential assembly strategies. Molecular Cell 2005;19:679–690. [PubMed: 16137623]
17. Reardon JT, Mu D, Sancar A. Overproduction. J Biol Chem 1997;27:19451–19456.
18. Reardon JT, Sancar A. Molecular anatomy of the human excision nuclease assembled at sites of DNA damage. Mol Cell Biol 2002;22:5938–5945. [PubMed: 12138203]
19. Reardon JT, Sancar A. Recognition and repair of the cyclobutane thymine dimer, a major cause of skin cancers, by the human excision nuclease. Genes Dev 2003;17:2539–2551. [PubMed: 14522951]
20. Reardon JT, Sancar A. Thermodynamic cooperativity and kinetic proofreading in DNA damage recognition and repair. Cell Cycle 2003;3(2):141–144. [PubMed: 14712076]
21. Sancar A, Lindsey-Boltz LA, Unsal-Kacmaz K, Linn S. Molecular mechanisms of mammalian DNA repair and the DNA damage checkpoints. Annu Rev Biochem 2004;73:39–85. [PubMed: 15189136]
22. Sugasawa K, Ng JMY, Masutani C, Iwai S, van der Spek PJ, Eker APM, Hanaoka F. Xeroderma pifmentosum group C protein complex in the initiator of global genome nucleotide excision repair. Mol Cell 1998;2:223–232. [PubMed: 9734359]
23. Volker M, Moné MJ, Karmakar P, van Hoffen A, Schul W, Vermeulen W, Hoeijmakers JHJ, van Driel R, van Zeeland AA, Mullenders LHF. Sequential assembly of the nucleotide excision repair factors in vivo. Mol Cell 2001;8:213–224. [PubMed: 11511374]
24. Wakasugi M, Sancar A. Assembly, subunit composition, and footprint of human DNA repair excision nuclease. Proc Natl Acad Sci 1998;95:6669–6674. [PubMed: 9618470]
25. Wakasugi M, Sancar A. Order of assembly of human DNA repair excision nuclease. J Biol Chem 1999;274:18759–18768. [PubMed: 10373492]
26. Wood RD. Nucleotide excision repair in mammalian cells. J Biol Chem 1997;272:23465–23468. [PubMed: 9295277]

7. Appendix 1 - Energy Constraints

In modeling the cooperativity of repair factors in excision repair, it is important to take into account the binding energy and insure that it is conserved. This is due to the fact that we model

cooperativity by changing the rate at which certain reactions occur effectively changing the relative binding energy before and after the reaction. If binding energy is not conserved we can end up in a situation like the left panel of Figure 10 where the energy of state C12 depends on which intermediate state it went through. The right panel of Figure 10 shows the correct way to balance the binding energy resulting in the same energy for state C12 no matter what intermediate steps are taken. Obeying this consideration results in a conservation of energy equation each time there are multiple paths from one state to another. These equations require that the products of association constants and cooperativity constants (for forward cooperativity) or the products of dissociation constants and cooperativity constants (for backward cooperativity) are the same along each path with the same beginning and ending states. The simplest way to model cooperativity and conserve binding energy is how it is done in this model where the cooperativity constant only depends on the number of repair factors in a complex rather than depending on which repair factor is a part of the complex. In the model equations (Appendix 2) backward cooperativity is shown.

8. Appendix 2 - Model Equations

These are the differential equations which constitute the excision repair model. The "*A*" complexes are DNA with no repair factors bound. The "*B*" and "*C*" complexes are DNA with one or two repair factors bound (the subscripts of these complexes indicate which proteins are bound - 1 being RPA, 2 being XPA, and 3 being XPC). The "*D*" complexes are DNA with all three repair factors (RPA, XPA, and XPC) bound. The "*E*" complexes are PIC1. The "*F*" complexes are PIC2 and the "*XP*" complexes are excised DNA. In all of these complexes the subscripts "*d*", "*u*", and "*m*" refer to damaged DNA, undamaged DNA, and damaged DNA on which the repair factors have assembled at the wrong location, respectively. The "c_{XXX}" variables are the concentration of the repair factor "XXX". "k_{co}" is the cooperativity constant (the model with backward cooperativity is shown in these equations). The association and dissociation constants are the "κ's", with the superscript indicating association ("*on*") or dissociation ("*off*") and the subscript indicating which repair factor the constant is for (the association constant is the same for all repair factors.

The first section of the model deals with the random order assembly of RPA, XPA, and XPC on the DNA. Equations 1–8 model the random order assembly of the repair factors on damaged portions of the DNA, equations 12–18 deal with repair factors that have bound to damaged DNA away from the lesion (repair factors which have missed the damage), and equations 22–29 show the assembly of repair factors on undamaged DNA. The other section of the model simulates the kinetic proofreading portion of excision repair. This is shown in equations 9–11 (damaged), equations 19–21 (missed), and equations 30–32 (undamaged). The remaining equations (33–37) are for the concentration of the various repair factors. The concentration of XPF doesn't change as this is the final step in the model, so XPF binding results in excision of the DNA and dissociation of the entire repair complex.

Random Order Assembly of Repair Factors on Damaged DNA

$$\begin{aligned}\frac{dA^d}{dt} = &-\kappa^{on}(c_{RPA}+c_{XPA}+c_{XPC})A^d+\kappa^{off,d}_{RPA}B^d_1+\kappa^{off,d}_{XPA}B^d_2\\&+\kappa^{off,d}_{XPC}B^d_3+\kappa^{off,u}_{RPA}B^m_1+\kappa^{off,u}_{XPA}B^m_2+\kappa^{off,u}_{XPC}B^m_3\\&+k^d_{pr}(k_1D^d+\kappa^{on}c_{XPG}E^d+\kappa^{on}c_{XPF}F^d)\end{aligned} \quad (1)$$

$$\frac{dB_1^d}{dt}=k_{co}\kappa_{XPA}^{off,d}C_{12}^d+k_{co}\kappa_{XPC}^{off,d}C_{13}^d+\kappa^{on}c_{RPA}A^dPr_{hit}-\left(\kappa_{RPA}^{off,d}+\kappa^{on}c_{XPA}+\kappa^{on}c_{XPC}\right)B_1^d \quad (2)$$

$$\frac{dB_2^d}{dt}=k_{co}\kappa_{RPA}^{off,d}C_{12}^d+k_{co}\kappa_{XPC}^{off,d}C_{23}^d+\kappa^{on}c_{XPA}A^dPr_{hit}-\left(\kappa_{XPA}^{off,d}+\kappa^{on}c_{RPA}+\kappa^{on}c_{XPC}\right)B_2^d \quad (3)$$

$$\frac{dB_3^d}{dt}=k_{co}\kappa_{XPA}^{off,d}C_{23}^d+k_{co}\kappa_{RPA}^{off,d}C_{13}^d+\kappa^{on}c_{XPC}A^dPr_{hit}-\left(\kappa_{XPC}^{off,d}+\kappa^{on}c_{RPA}+\kappa^{on}c_{XPA}\right)B_3^d \quad (4)$$

$$\frac{dC_{12}^d}{dt}=\kappa^{on}(c_{RPA}B_2^d+c_{XPA}B_1^d-c_{XPC}C_{12}^d)-\left(\kappa_{RPA}^{off,d}+\kappa_{XPA}^{off,d}\right)k_{co}C_{12}^d+k_{co}^2\kappa_{XPC}^{off,d}D^d \quad (5)$$

$$\frac{dC_{13}^d}{dt}=\kappa^{on}(c_{RPA}B_3^d+c_{XPC}B_1^d-c_{XPA}C_{13}^d)-\left(\kappa_{RPA}^{off,d}+\kappa_{XPC}^{off,d}\right)k_{co}C_{13}^d+k_{co}^2\kappa_{XPA}^{off,d}D^d \quad (6)$$

$$\frac{dC_{23}^d}{dt}=\kappa^{on}(c_{XPC}B_2^d+c_{XPA}B_3^d-c_{RPA}C_{23}^d)-\left(\kappa_{XPC}^{off,d}+\kappa_{XPA}^{off,d}\right)k_{co}C_{23}^d+k_{co}^2\kappa_{RPA}^{off,d}D^d \quad (7)$$

$$\frac{dD^d}{dt}=\kappa^{on}(c_{XPC}C_{12}^d+c_{XPA}C_{13}^d+c_{RPA}C_{23}^d)-\left(\kappa_{XPC}^{off,d}+\kappa_{XPA}^{off,d}+\kappa_{RPA}^{off,d}\right)k_{co}^2D^d-k_1D^d \quad (8)$$

Kinetic Proofreading of Repair Complexes on Damaged DNA

$$\frac{dE^d}{dt}=k_1(1-k_{Pr}^d)D^d-\kappa^{on}c_{XPG}E^d \quad (9)$$

$$\frac{dF^d}{dt}=(1-k_{Pr}^d)\kappa^{on}c_{XPG}E^d-\kappa^{on}c_{XPF}F^d \quad (10)$$

$$\frac{dXP^d}{dt} = (1 - k_{Pr}^d)\kappa^{on} c_{XPF} F^d \tag{11}$$

Random Order Assembly of Repair Factors Away From Lesions on Damaged DNA

$$\frac{dB_1^m}{dt} = k_{co}\kappa_{XPA}^{off,u} C_{12}^m + k_{co}\kappa_{XPC}^{off,u} C_{13}^m + \kappa^{on} c_{RPA} A^d (1 - Pr_{hit}) - \left(\kappa_{RPA}^{off,u} + \kappa^{on} c_{XPA} + \kappa^{on} c_{XPC}\right) B_1^m \tag{12}$$

$$\frac{dB_2^m}{dt} = k_{co}\kappa_{RPA}^{off,u} C_{12}^m + k_{co}\kappa_{XPC}^{off,u} C_{23}^m + \kappa^{on} c_{XPA} A^d (1 - Pr_{hit}) - \left(\kappa_{XPA}^{off,u} + \kappa^{on} c_{RPA} + \kappa^{on} c_{XPC}\right) B_2^m \tag{13}$$

$$\frac{dB_3^m}{dt} = k_{co}\kappa_{XPA}^{off,u} C_{23}^m + k_{co}\kappa_{RPA}^{off,u} C_{13}^m + \kappa^{on} c_{XPC} A^d (1 - Pr_{hit}) - \left(\kappa_{XPC}^{off,u} + \kappa^{on} c_{RPA} + \kappa^{on} c_{XPA}\right) B_3^m \tag{14}$$

$$\frac{dC_{12}^m}{dt} = \kappa^{on}(c_{RPA} B_2^m + c_{XPA} B_1^m - c_{XPC} C_{12}^m) - \left(\kappa_{RPA}^{off,u} + \kappa_{XPA}^{off,u}\right) k_{co} C_{12}^m + k_{co}^2 \kappa_{XPC}^{off,u} D^m \tag{15}$$

$$\frac{dC_{13}^m}{dt} = \kappa^{on}(c_{RPA} B_3^m + c_{XPC} B_1^m - c_{XPA} C_{13}^m) - \left(\kappa_{RPA}^{off,u} + \kappa_{XPC}^{off,u}\right) k_{co} C_{13}^m + k_{co}^2 \kappa_{XPA}^{off,u} D^m \tag{16}$$

$$\frac{dC_{23}^m}{dt} = \kappa^{on}(c_{XPC} B_2^m + c_{XPA} B_3^m - c_{RPA} C_{23}^m) - \left(\kappa_{XPC}^{off,u} + \kappa_{XPA}^{off,u}\right) k_{co} C_{23}^m + k_{co}^2 \kappa_{RPA}^{off,u} D^m \tag{17}$$

$$\frac{dD^m}{dt} = \kappa^{on}(c_{XPC} C_{12}^m + c_{XPA} C_{13}^m - c_{RPA} C_{23}^m) - \left(\kappa_{XPC}^{off,u} + \kappa_{XPA}^{off,u} + \kappa_{RPA}^{off,u}\right) k_{co}^2 D^m - k_1 D^m \tag{18}$$

Kinetic Proofreading on Repair Complexes Formed Away From Lesions on Damaged DNA

$$\frac{dE^m}{dt} = k_1(1 - k_{Pr}^m) D^m - \kappa^{on} c_{XPG} E^m \tag{19}$$

$$\frac{dF^m}{dt} = (1 - k_{Pr}^m)\kappa^{on} c_{XPG} E^m - \kappa^{on} c_{XPF} F^m \tag{20}$$

$$\frac{dXP^m}{dt} = (1 - k_{Pr}^m)\kappa^{on} c_{XPF} F^m \tag{21}$$

Random Order Assembly of Repair Factors on Undamaged DNA

$$\frac{dA^u}{dt} = -\kappa^{on}(c_{RPA} + c_{XPA} + c_{XPC})A^u + \kappa_{RPA}^{off,u} B_1^u + \kappa_{XPA}^{off,u} B_2^u + \kappa_{XPC}^{off,u} B_3^u + k_{pr}^u (k_1 D^u + \kappa^{on} c_{XPG} E^u + \kappa^{on} c_{XPF} F^u) \tag{22}$$

$$\frac{dB_1^u}{dt} = k_{co}\kappa_{XPA}^{off,u} C_{12}^u + k_{co}\kappa_{XPC}^{off,u} C_{13}^u + \kappa^{on} c_{RPA} A^u - \left(\kappa_{RPA}^{off,u} + \kappa^{on} c_{XPA} + \kappa^{on} c_{XPC}\right) B_1^u \tag{23}$$

$$\frac{dB_2^u}{dt} = k_{co}\kappa_{RPA}^{off,u} C_{12}^u + k_{co}\kappa_{XPC}^{off,u} C_{23}^u + \kappa^{on} c_{XPA} A^u - \left(\kappa_{XPA}^{off,u} + \kappa^{on} c_{RPA} + \kappa^{on} c_{XPC}\right) B_2^u \tag{24}$$

$$\frac{dB_3^u}{dt} = k_{co}\kappa_{XPA}^{off,u} C_{23}^u + k_{co}\kappa_{RPA}^{off,u} C_{13}^u + \kappa^{on} c_{XPC} A^u - \left(\kappa_{XPC}^{off,u} + \kappa^{on} c_{RPA} + \kappa^{on} c_{XPA}\right) B_3^u \tag{25}$$

$$\frac{dC_{12}^u}{dt} = \kappa^{on}(c_{RPA} B_2^u + c_{XPA} B_1^u - c_{XPC} C_{12}^u) - \left(\kappa_{RPA}^{off,u} + \kappa_{XPA}^{off,u}\right) k_{co} C_{12}^u + k_{co}^2 \kappa_{XPC}^{off,u} D^u \tag{26}$$

$$\frac{dC_{13}^u}{dt} = \kappa^{on}(c_{RPA} B_3^u + c_{XPC} B_1^u - c_{XPA} C_{13}^u) - \left(\kappa_{RPA}^{off,u} + \kappa_{XPC}^{off,u}\right) k_{co} C_{13}^u + k_{co}^2 \kappa_{XPA}^{off,u} D^u \tag{27}$$

$$\frac{dC_{23}^u}{dt} = \kappa^{on}(c_{XPC} B_2^u + c_{XPA} B_3^u - c_{RPA} C_{23}^u) - \left(\kappa_{XPC}^{off,u} + \kappa_{XPA}^{off,u}\right) k_{co} C_{23}^u + k_{co}^2 \kappa_{RPA}^{off,u} D^u \tag{28}$$

$$\frac{dD^u}{dt} = \kappa^{on}(c_{XPC} C_{12}^u + c_{XPA} C_{13}^u - c_{RPA} C_{23}^u) - \left(\kappa_{XPC}^{off,u} + \kappa_{XPA}^{off,u} + \kappa_{RPA}^{off,u}\right) k_{co}^2 D^u - k_1 D^u \tag{29}$$

Kinetic Proofreading of Repair Complexes on Undamaged DNA

$$\frac{dE^u}{dt} = k_1(1 - k^u_{Pr})D^u - \kappa^{on} c_{XPG} E^u \tag{30}$$

$$\frac{dF^u}{dt} = (1 - k^u_{Pr})\kappa^{on} c_{XPG} E^u - \kappa^{on} c_{XPF} F^u \tag{31}$$

$$\frac{dXP^u}{dt} = (1 - k^u_{Pr})\kappa^{on} c_{XPF} F^u \tag{32}$$

$$\begin{aligned}\frac{dc_{RPA}}{dt} &= \kappa^{off,d}_{RPA}(B^d_1 + k_{co}(C^d_{12} + C^d_{13} + k_{co}D^d)) \\ &+ \kappa^{off,u}_{RPA}(B^u_1 + B^m_1 + k_{co}(C^u_{12} + C^u_{13} + k_{co}D^u + C^m_{12} + C^m_{13} + k_{co}D^m)) \\ &- \kappa^{on} c_{RPA}(A^d + B^d_2 + B^d_3 + C^d_{23} + B^m_2 + B^m_3 + C^m_{23} + A^u + B^u_2 + B^u_3 + C^u_{23}) \\ &+ k_1(k^d_{Pr} D^d + k^u_{Pr}(D^m + D^u)) + \kappa^{on} c_{XPG}(k^d_{Pr} E^d + k^u_{Pr}(E^m + E^u)) \\ &+ \kappa^{on} c_{XPF}(F^d + F^m + F^u)\end{aligned} \tag{33}$$

$$\begin{aligned}\frac{dc_{XPA}}{dt} &= \kappa^{off,d}_{XPA}(B^d_2 + k_{co}(C^d_{12} + C^d_{23} + k_{co}D^d)) \\ &+ \kappa^{off,u}_{XPA}(B^u_2 + B^m_2 + k_{co}(C^u_{12} + C^u_{23} + k_{co}D^u + C^m_{12} + C^m_{23} + k^2_{co}D^m)) \\ &- \kappa^{on} c_{XPA}(A^d + B^d_1 + B^d_3 + C^d_{13} + B^m_1 + B^m_3 + C^m_{13} + A^u + B^u_1 + B^u_3 + C^u_{13}) \\ &+ k_1(k^d_{Pr} D^d + k^u_{Pr}(D^m + D^u)) + \kappa^{on} c_{XPG}(k^d_{Pr} E^d + k^u_{Pr}(E^m + E^u)) \\ &+ \kappa^{on} c_{XPF}(F^d + F^m + F^u)\end{aligned} \tag{34}$$

$$\begin{aligned}\frac{dc_{XPC}}{dt} &= \kappa^{off,d}_{XPC}(B^d_3 + k_{co}(C^d_{13} + C^d_{23} + k_{co}D^d)) \\ &+ \kappa^{off,u}_{XPC}(B^u_3 + B^m_3 + k_{co}(C^u_{13} + C^u_{23} + k_{co}D^u + C^m_{13} + C^m_{23} + k_{co}D^m)) \\ &- \kappa^{on} c_{XPC}(A^d + B^d_1 + B^d_2 + C^d_{12} + B^m_1 + B^m_2 + C^m_{12} + A^u + B^u_1 + B^u_2 + C^u_{12}) \\ &+ k_1(k^d_{Pr} D^d + k^u_{Pr}(D^m + D^u)) + \kappa^{on} c_{XPG}(k^d_{Pr} E^d + k^u_{Pr}(E^m + E^u)) \\ &+ \kappa^{on} c_{XPF}(F^d + F^m + F^u)\end{aligned} \tag{35}$$

$$\frac{dc_{XPG}}{dt} = -\kappa_{on} c_{XPG}((1 - k^d_{Pr})E^d + (1 - k^u_{Pr})(E^m + E^u)) + \kappa_{on} c_{XPF}(F^d + F^m + F^u) \tag{36}$$

$$\frac{dc_{XPF}}{dt} = 0 \tag{37}$$

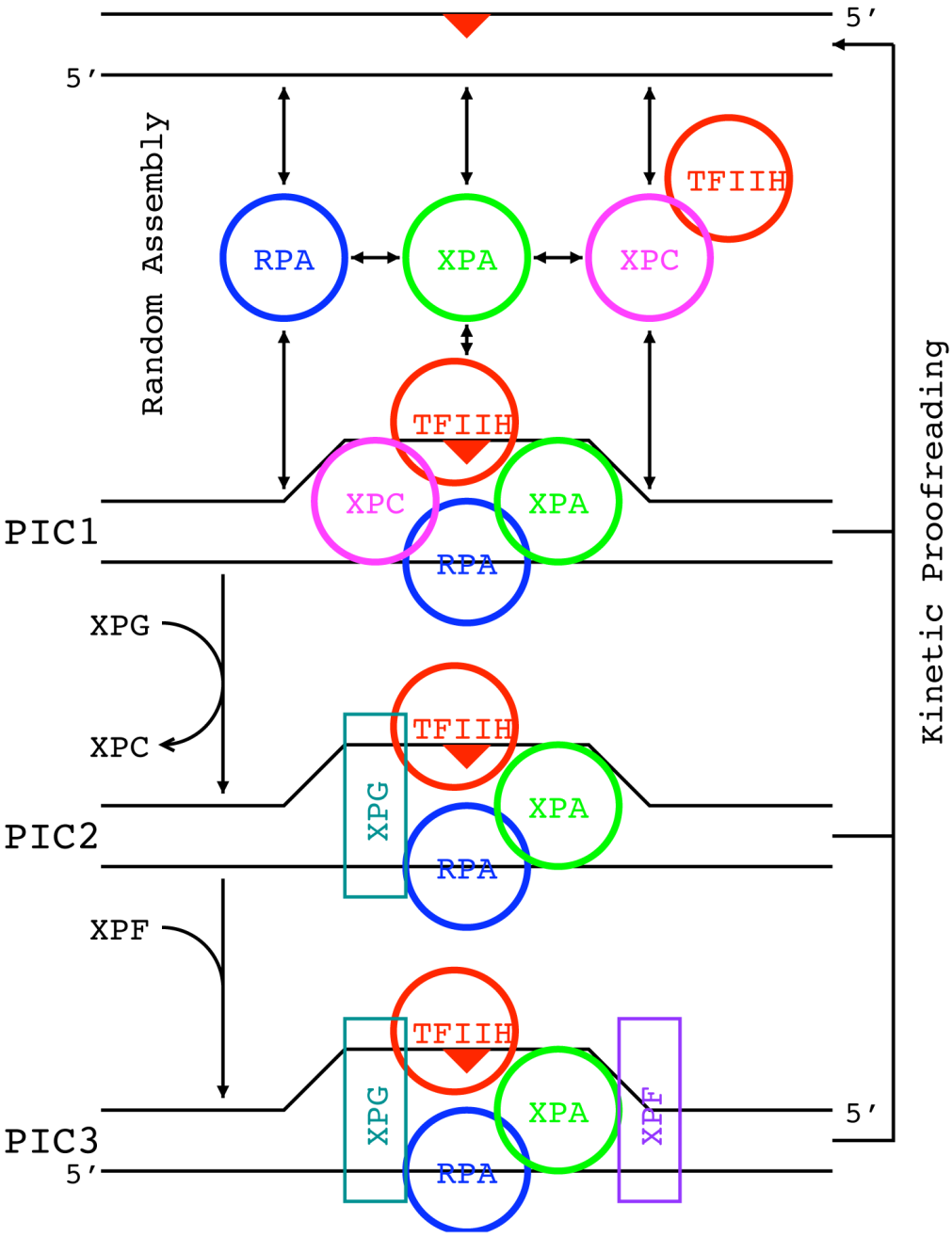

Figure 1.
Schematic of Nucleotide Excision Repair. This figure shows a schematic diagram representing how excision repair is assumed to operate in the random order cooperative assembly and kinetic proofreading model of human excision repair.

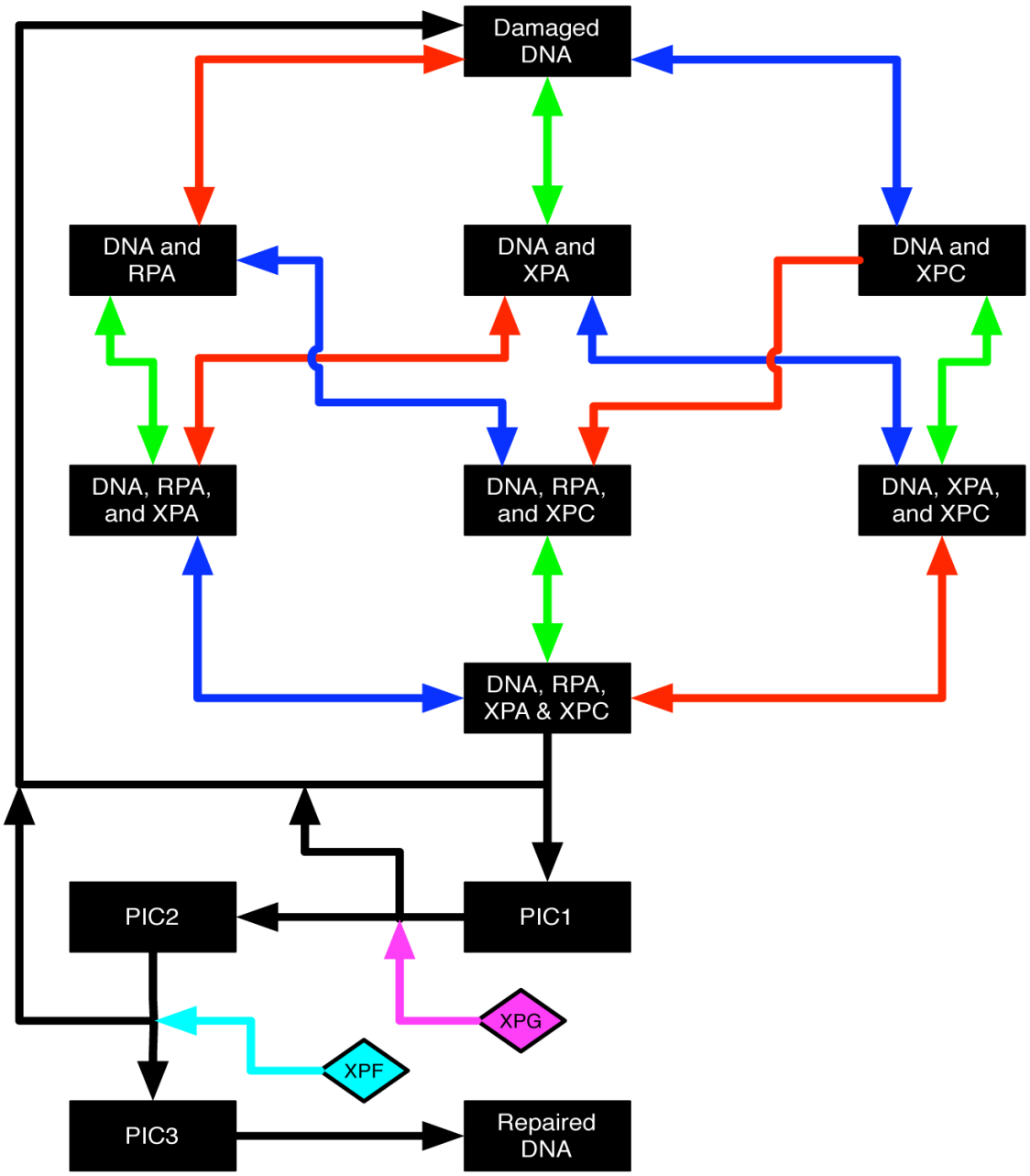

Figure 2.
Schematic of the Nucleotide Excision Repair model. This figure shows a schematic diagram of the allowable states of the DNA substrate in the model and how they can evolve.

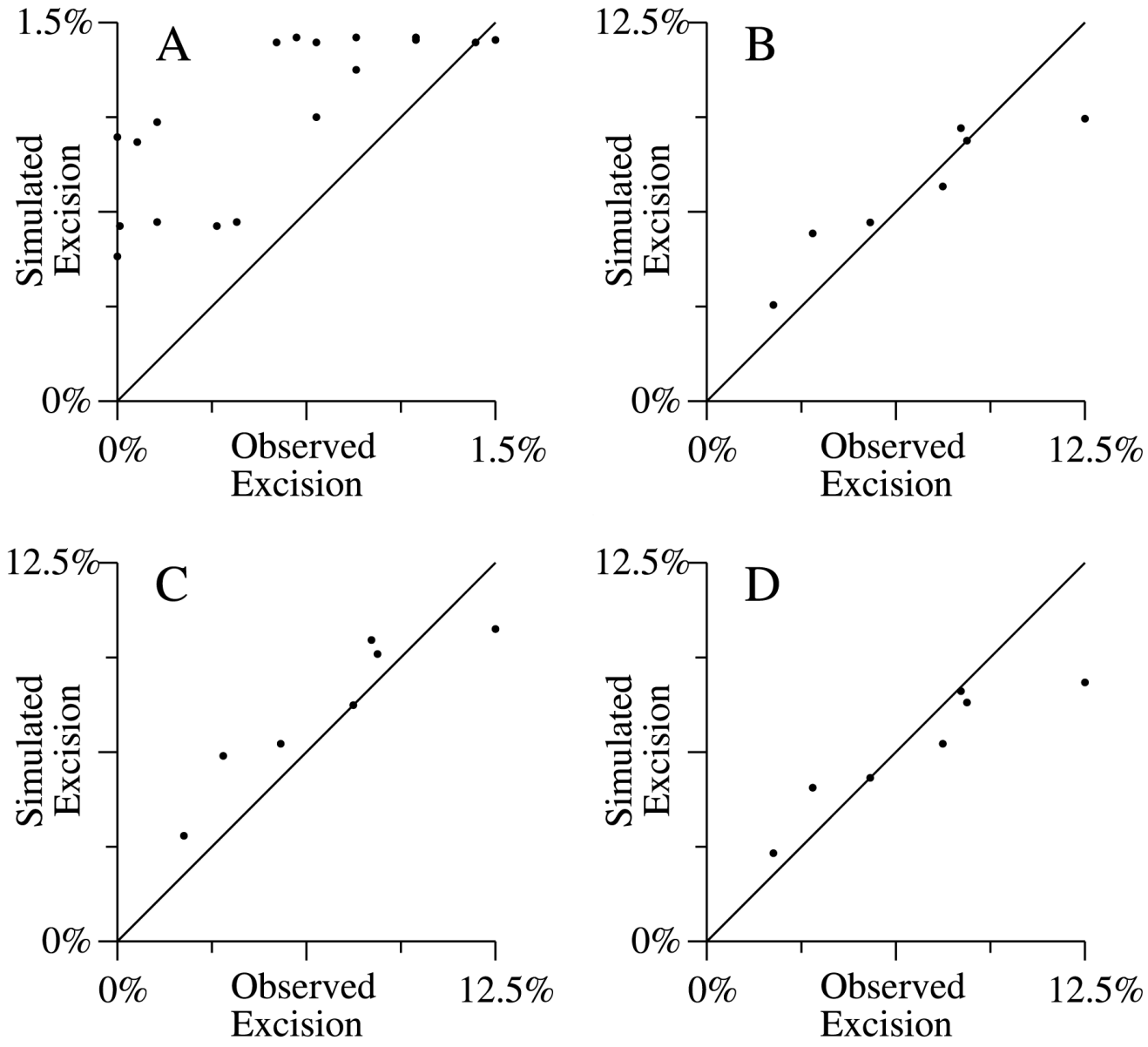

Figure 3.

Scatter plots – these panels show results with the model tuned to results from experiments with T<>T dimers (panel A) (Table 4, run 2a) and (6 – 4) photoproducts (Table 5, runs 1 (panel C), 2a (panel B), and 3c (panel D). Each of these panels compares output from the model with experimental results. Each point represents the amount of DNA excision observed in an experiment (the x-coordinate) and the amount excised in a simulation of the experiment using the model (the y-coordinate). The maximal observed excision was 1.5% for T<>T dimers and 12.5% for (6 – 4) photoproducts.

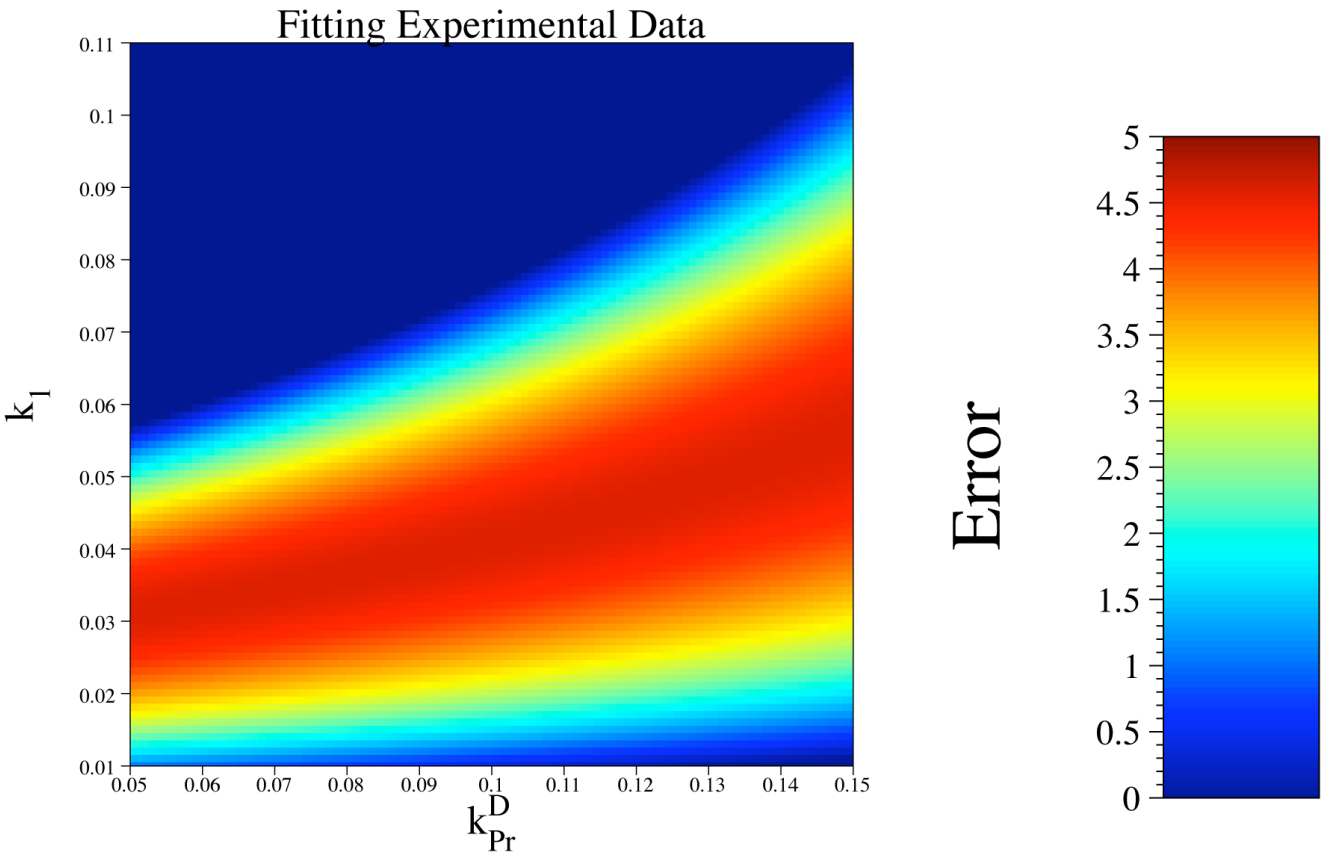

Figure 4.

The total normalized squared error from simulating seven different runs from Table 5. The color indicates the error with red being 0 and blue being 5 as shown in the color scale to the right of the figure. The parameters being varied are k_{Pr}^{D}, the probability that kinetic proofreading mistakenly dissociates the complex from damaged DNA, and k_1, the rate at which the complex with all three repair factors undergoes kinetic proofreading. The horizontal axis indicates the variable k_{Pr}^{D} (ranging from 0.05 to 0.15) and the vertical axis indicates the parameter k_1 (ranging from 0.01 to 0.11). Seven different experiments were conducted with each pair of parameter values and the error between the simulations and experiments was calculated.

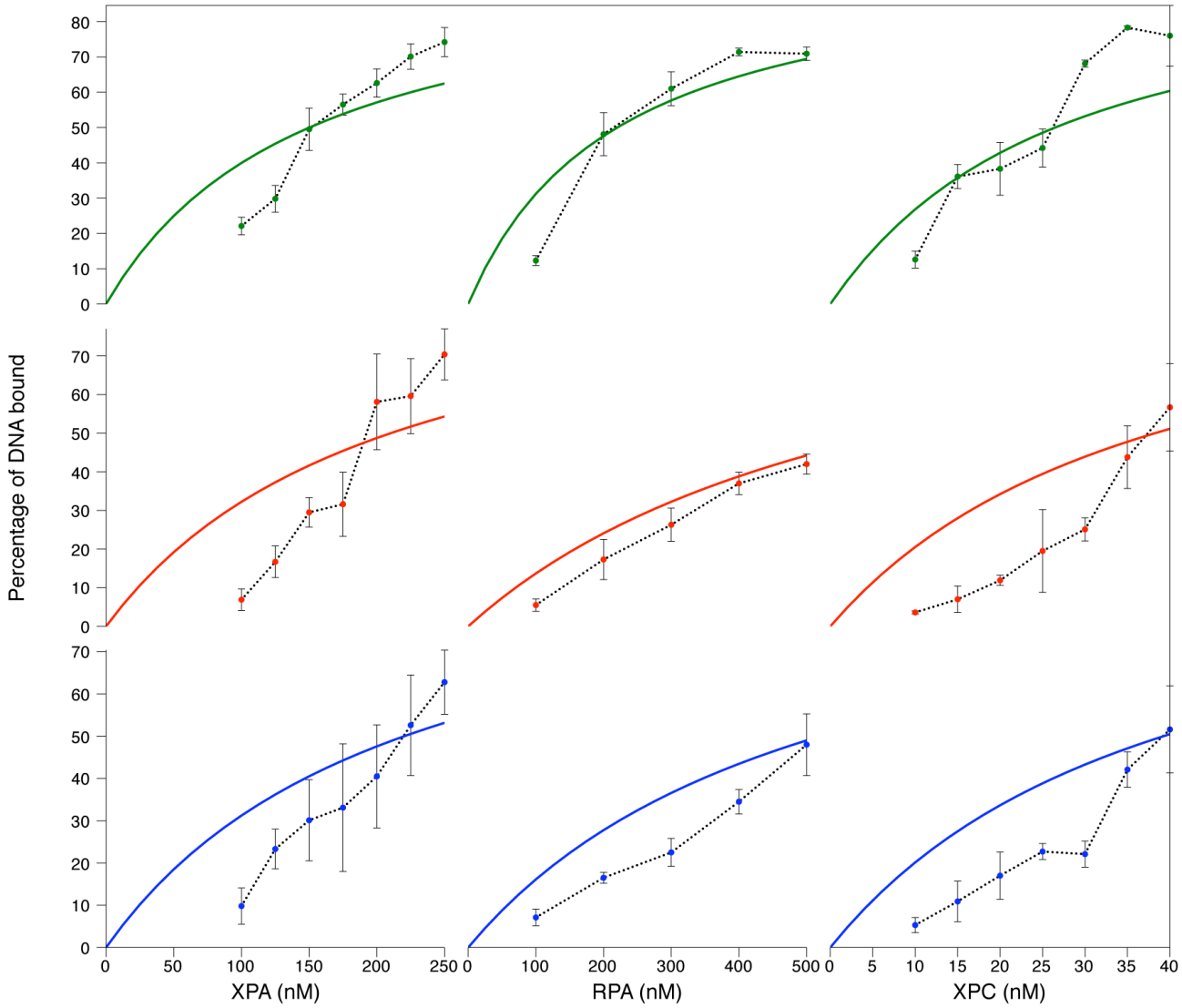

Figure 5.

Repair factor binding isotherms: This figure shows the results of a simulation that models the experiment to determine the dissociation constant for all three repair factors. The percentage of each repair factor bound to DNA vs. the concentration of the repair factor was plotted for undamaged DNA (blue), the *T* <> *T* dimer (red), and the 6–4 photoproduct (green). The filled circles connect by dotted lines are experimental results (with error bars), the lines simulated results.

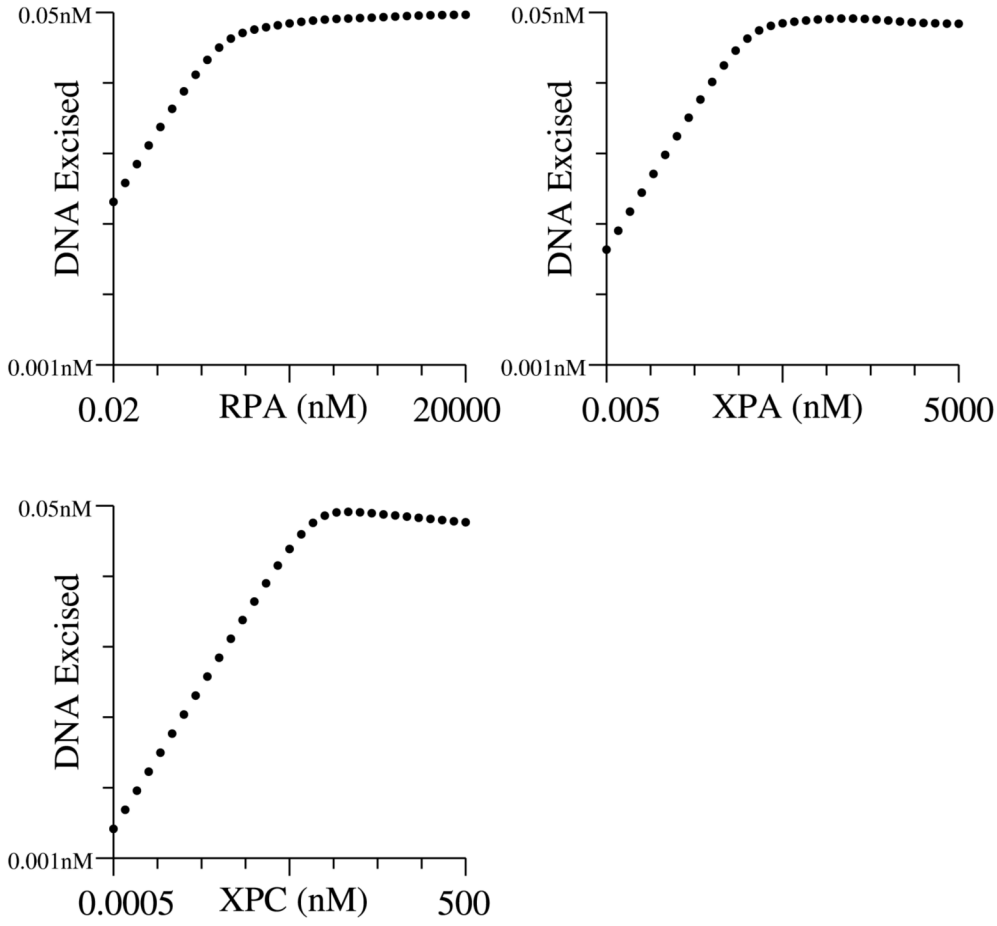

Figure 6.

Effect of concentrations of damage recognition factors on repair rate: Each panel shows the effects of varying the concentration of the indicated repair factor on the simulated amount of DNA excised. Each repair factor is varied from 10^{-4} to 10^{2} times the baseline value while holding the concentrations of the other repair factors constant (the y-axis is a log scale varying from 10^{-3}nM to 5×10^{-2}nM).

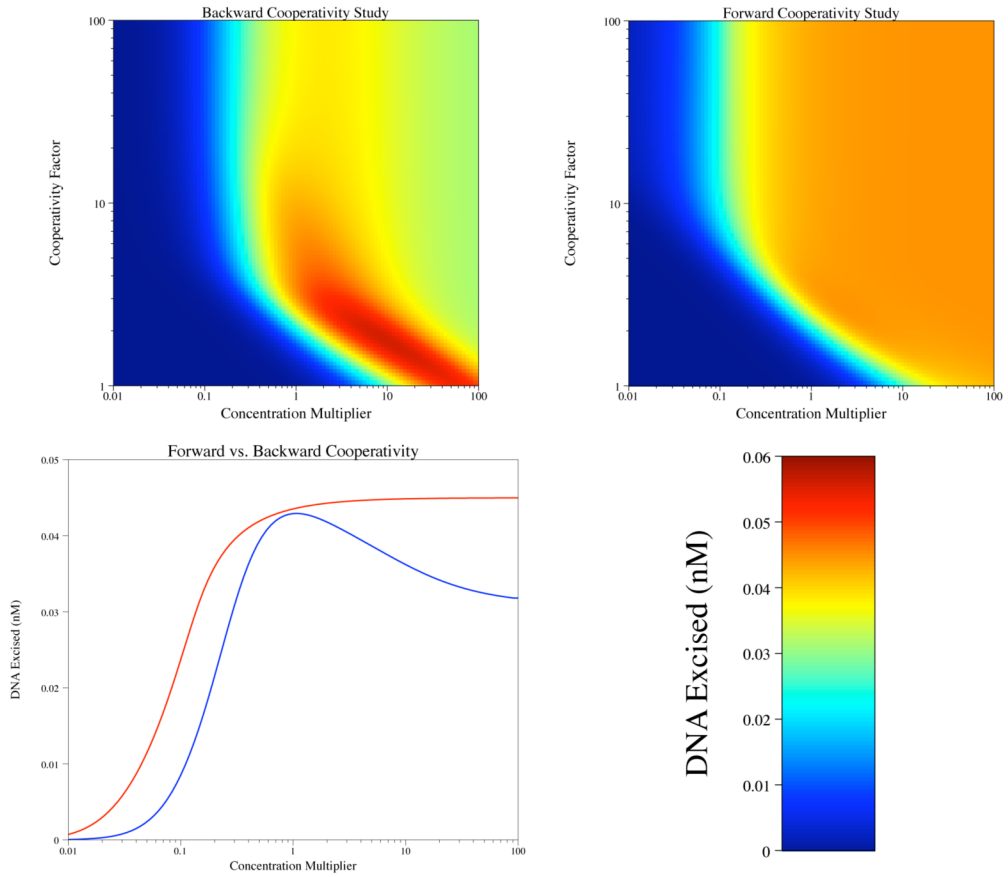

Figure 7.

Cooperativity study: This figure shows how cooperativity affects excision in the model. In the upper 2 panels the x-axis gives the concentration of the repair factors (which range from 10^{-2} to 10^{2} times the baseline values) and the y-axis gives the value of the cooperativity constant (which ranges from 1 to 100). The color indicates the amount of excision with blue being low and red being high as shown in the color scale in the lower right frame. The upper left frame is the backward cooperativity study and the upper right frame is the forward cooperativity study. The lower left frame is a comparison of the forward cooperativity model (red) and the backward cooperativity model (blue) for a cooperativity constant of 10 in both models.

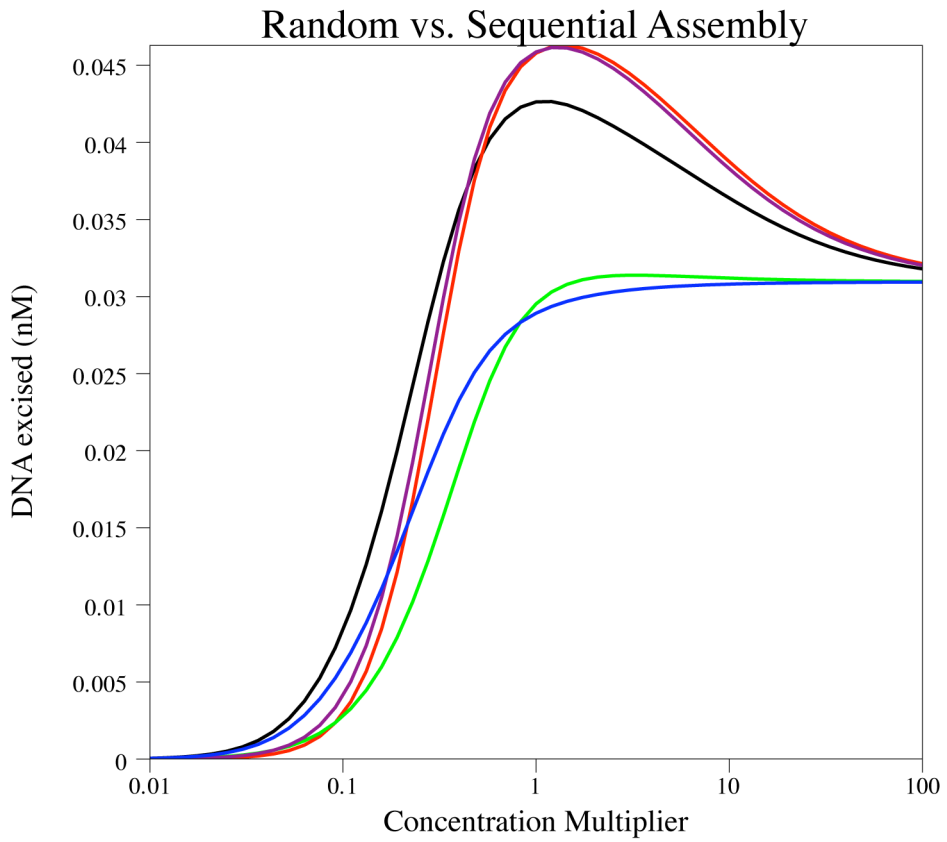

Figure 8.

Random vs. sequential assembly: This figure shows the effect of changing the concentration of repair factors on the amount of (6–4) PP excised for five different configurations of the model: Black is the standard random order assembly model; Red is the sequential model in which the order of binding is RPA, XPA, then XPC; Green is the sequential model where the order of binding was XPC, XPA, then RPA; Purple is the hybrid model where RPA is required to bind first; and Blue is the hybrid model where XPC is required to bind first.

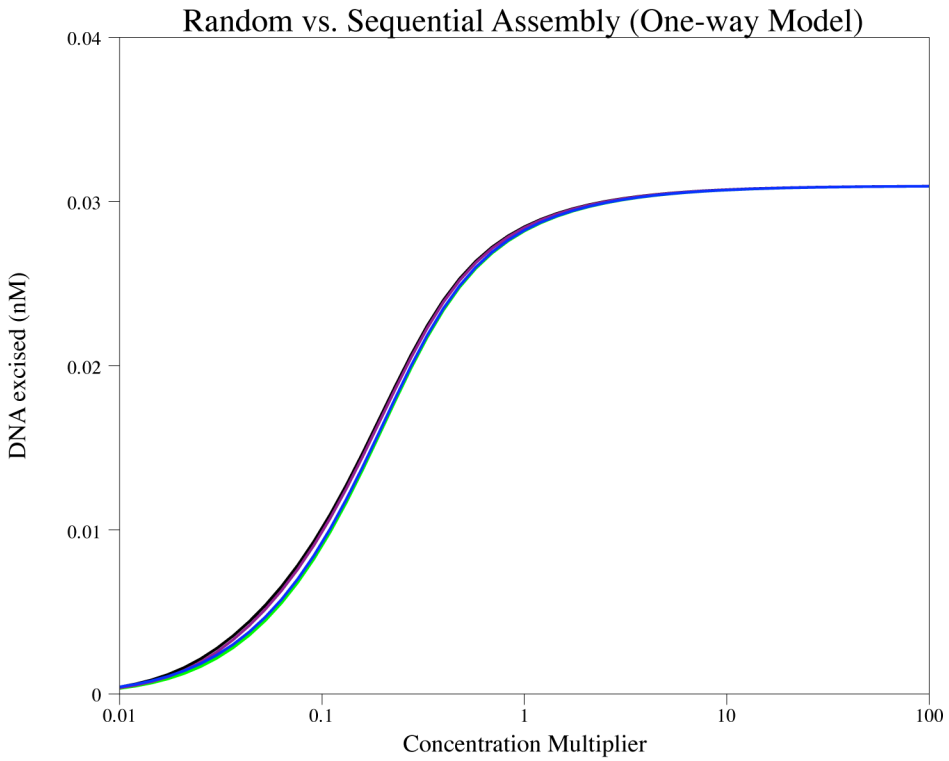

Figure 9.

Random vs. sequential assembly: This figure shows the effect of changing the concentration of repair factors on the amount of (6–4) PP excised for five different configurations of the model: Black is the standard random order assembly model; Red is the sequential model in which the order of binding is RPA, XPA, then XPC; Green is the sequential model where the order of binding was XPC, XPA, then RPA; Purple is the hybrid model where RPA is required to bind first; and Blue is the hybrid model where XPC is required to bind first. All of the models in this study were one-way (i.e., repair factors once bound could not dissociate).

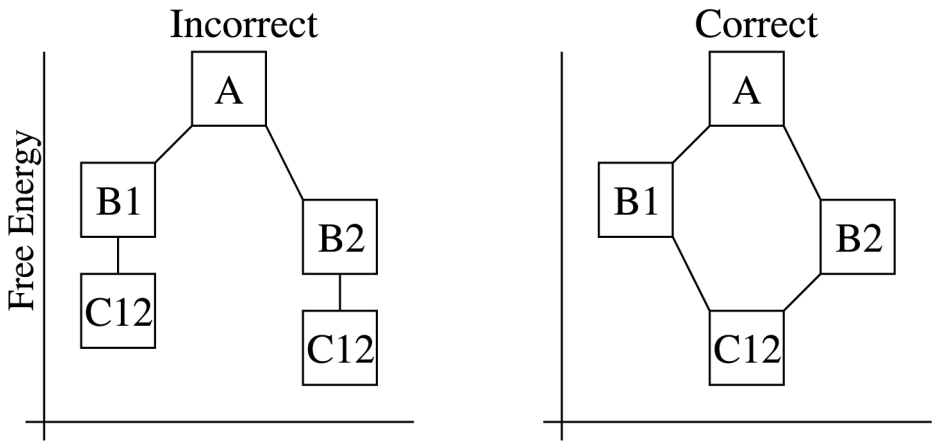

Figure 10.

Example of free energy considerations for modeling cooperativity. This figure shows the correct (right) and incorrect (left) ways of handling energy considerations when modeling cooperativity. In both panels complex A represents DNA alone, complexes B_1 and B_2 represent DNA with RPA or XPA respectively bound to DNA, and complex C_{12} represents DNA with RPA and XPA bound to DNA.

Table 1

Values of model constants

Constant	Value
κ_{on}	$10^6/(s \cdot M)$
κ_{RPA}^{64off}	$2.2 \cdot 10^{-7}$
κ_{XPA}^{64off}	$1.5 \cdot 10^{-7}$
κ_{XPC}^{64off}	$2.6 \cdot 10^{-8}$
κ_{RPA}^{TToff}	$6.3 \cdot 10^{-7}$
κ_{XPA}^{TToff}	$2.1 \cdot 10^{-7}$
κ_{XPC}^{TToff}	$3.8 \cdot 10^{-8}$
κ_{RPA}^{uoff}	$5.2 \cdot 10^{-7}$
κ_{XPA}^{uoff}	$2.2 \cdot 10^{-7}$
κ_{XPC}^{uoff}	$3.9 \cdot 10^{-8}$

Table 2

Values of model parameters

Paramter	Baseline
Pr_{hit}	0.3
k_{Pr}^{D}	0.1
k_{Pr}^{U}	0.9
k_1	0.06
Coop	0.01

Table 3

Sensitivity Results

Parameter	Sensitivity	Baseline	Range	Low	High
k_1	0.99	6.0×10^{-2}	$\pm 5 \times 10^{-3}$	0.0397	0.0468
Coop	0.65	0.01	±0.005	0.0415	0.0443
k_{On}	12.94	1.0×10^{6}	$\pm 5 \times 10^{5}$	0.0155	0.0714
k_{Pr}^{D}	−3.31	0.1	±0.05	0.0508	0.0365
k_{Pr}^{U}	0.00875	0.9	±0.05	0.043249	0.043291
Pr^{H}	0.44	0.3	±0.05	0.0375	0.0438

Table 4

Excision assays using the T<>T dimer

Run	c_{RPA}	c_{XPA}	c_{XPC}	c_{TFIIH}	Time	Excision
1	200	65	2.5	12.5	60	1.0 %
2a	200	65	2.5	12.5	90	1.8 %
2b	150	65	2.5	12.5	90	1.9 %
2c	100	65	2.5	12.5	90	1.5 %
2d	50	65	2.5	12.5	90	1.5 %
3a	50	130	2.5	12.5	90	1.2 %
3b	50	98	2.5	12.5	90	0.9 %
3c	50	65	2.5	12.5	90	1.2 %
3d	50	32	2.5	12.5	90	1.0 %
4a	50	32	2.5	12.5	90	0.8 %
4b	50	32	1.8	12.5	90	1.2 %
4c	50	32	1.2	12.5	90	1.0 %
4d	50	32	0.6	12.5	90	0.6 %
5a	50	32	0.6	12.5	90	0.5 %
5b	50	32	0.6	9.3	90	0.5 %
5c	50	32	0.6	6.2	90	0.3 %
5d	50	32	0.6	3.1	90	0.2 %
6a	34	32	1.2	6.2	90	0.2 %
6b	17	32	1.2	6.2	90	0.0 %
6c	34	16	1.2	6.2	90	0.1 %
6d	34	32	0.6	6.2	90	0.001 %
6e	17	16	0.6	6.2	90	0.0 %
6f	50	32	0.6	6.2	90	0.2 %
7	34	32	0.6	6.2	90	0.5 %
8a	50	32	0.6	6.2	90	0.1 %
8b	34	32	0.6	6.2	90	0.1 %
8c	34	32	1.2	6.2	90	0.15 %
8d	34	16	1.2	6.2	90	0.2 %
8e	17	32	1.2	6.2	90	0.0 %

Run	c_{RPA}	c_{XPA}	c_{XPC}	c_{TFIIH}	Time	Excision
8f	17	16	0.6	6.2	90	0.0 %
9a	200	65	2.5	12.5	90	1.8 %
9b	34	32	1.2	6.2	90	0.7 %

Table 5

Excision assays using the 6–4 photoproduct

Run	c_{RPA}	c_{XPA}	c_{XPC}	c_{TFIIH}	Time	Excision
1	34	32	1.2	6.2	90	7.8 %
2a	100	5.0	5	12.5	90	8.6 %
2b	100	12.5	5	12.5	90	8.4 %
2c	100	25	5	12.5	90	12.5 %
3a	200	1	5	12.5	60	2.2 %
3b	200	10	5	12.5	60	3.5 %
3c	200	50	5	12.5	60	5.4 %